

**Supplemental information**

**Characterizing the genetic architecture of drug  
response using gene-context interaction methods**

**Michal Sadowski, Mike Thompson, Joel Mefford, Tanushree Haldar, Akinyemi Oni-Orisan, Richard Border, Ali Pazokitoroudi, Na Cai, Julien F. Ayroles, Sriram Sankararaman, Andy W. Dahl, and Noah Zaitlen**

# Contents

## 1 Supplemental Figures

## 2 Supplemental Tables

## 3 Supplemental Note

- 3.1 Variance decomposition analysis with GxEMM
  - 3.1.1 The GxEMM model
  - 3.1.2 Using GxEMM to estimate treatment response heritability
  - 3.1.3 Negative estimates of drug-specific genetic variance
  - 3.1.4 Dependence of heritability estimates on covariates
- 3.2 TxEWAS for detection of gene-drug interactions
  - 3.2.1 The TxEWAS model
  - 3.2.2 TxEWAS performance in simulations
  - 3.2.3 Combinations of treatments
- 3.3 Endogeneity bias
  - 3.3.1 Simulating endogenous “E”
- 3.4 The impact of gene-drug interactions on polygenic prediction accuracy

## Supplemental References

# 1 Supplemental Figures

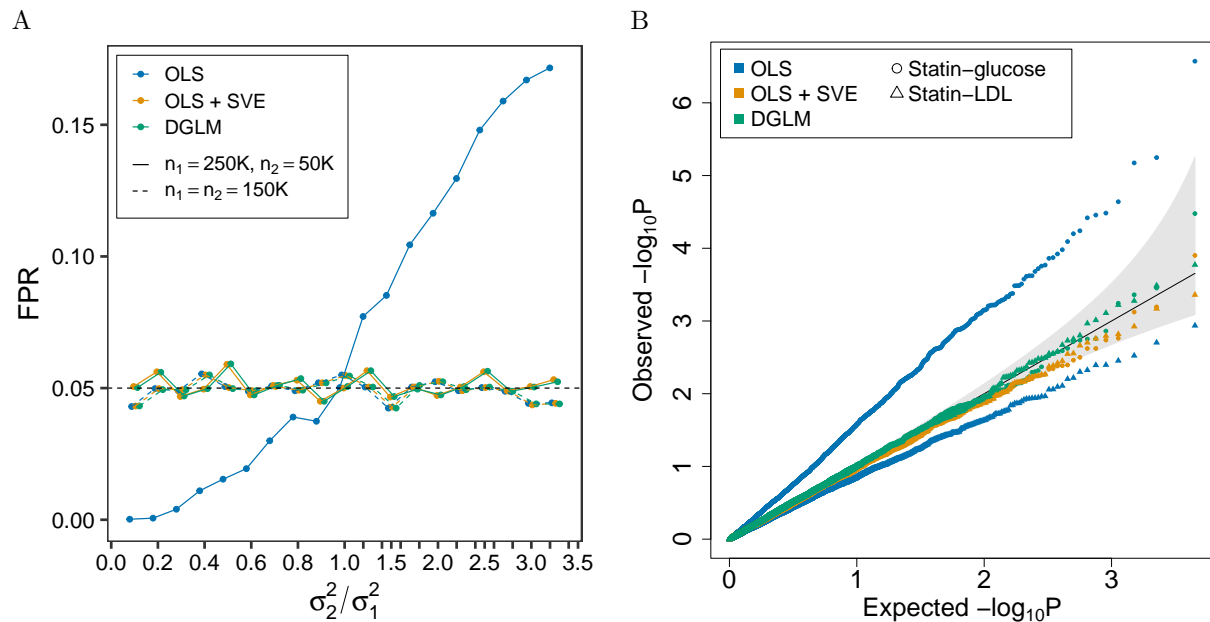


Figure S1. Evaluation of the type I error rate for the GxE effect estimated with the OLS model, the OLS model using robust standard errors (OLS + SVE) and the DGLM; related to Figure 1 and STAR Methods. (A) False positive rate (FPR) of GxE as a function of the ratio between phenotype variances in two environments: unexposed (of size  $n_1$  and phenotype variance  $\sigma_1^2$ ), and exposed (of size  $n_2$  and phenotype variance  $\sigma_2^2$ ). The nominal FPR of 5% is marked by the black dashed line. (B) Quantile-quantile plot comparing the null expected  $p$  values (x-axis) to the observed GxE  $p$  values after permuting real data from the UK Biobank (y-axis). The permutation permutes imputed expression of 4,516 genes and then tests their interaction with statins on blood glucose (circles) or LDL cholesterol (triangles).

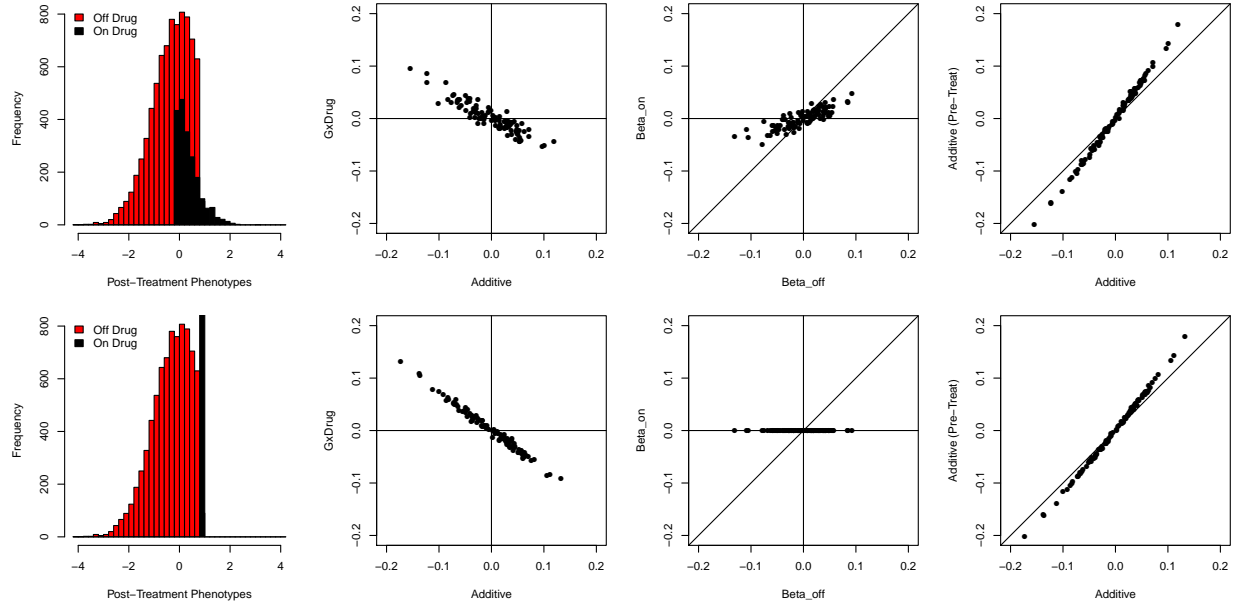


Figure S2. Endogeneity bias simulations; related to Figure 3. Top row: Simulation assumes that treatments have an equal additive effect on all individuals. Bottom row: Simulation assumes that treatments return all individuals to the treatment threshold, regardless their initial phenotypes. First column: Cross-sectional phenotype distribution, stratified by treatment status. Second column: Comparison of estimated additive vs interaction effect sizes. Third column: Comparison of estimated effect sizes in treated vs untreated individuals. Fourth column: comparison of additive effect estimated on pre-treatment phenotypes vs cross-sectionally observed phenotypes containing a mix of treated and untreated individuals.

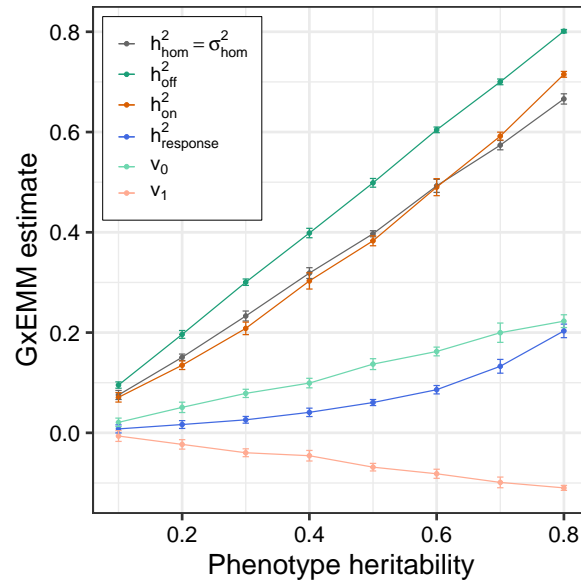


Figure S3. GxEMM estimates in the presence of the buffering effect of a drug; related to Table 2 and Figure 3. Error bars represent standard deviation over 10 simulations.



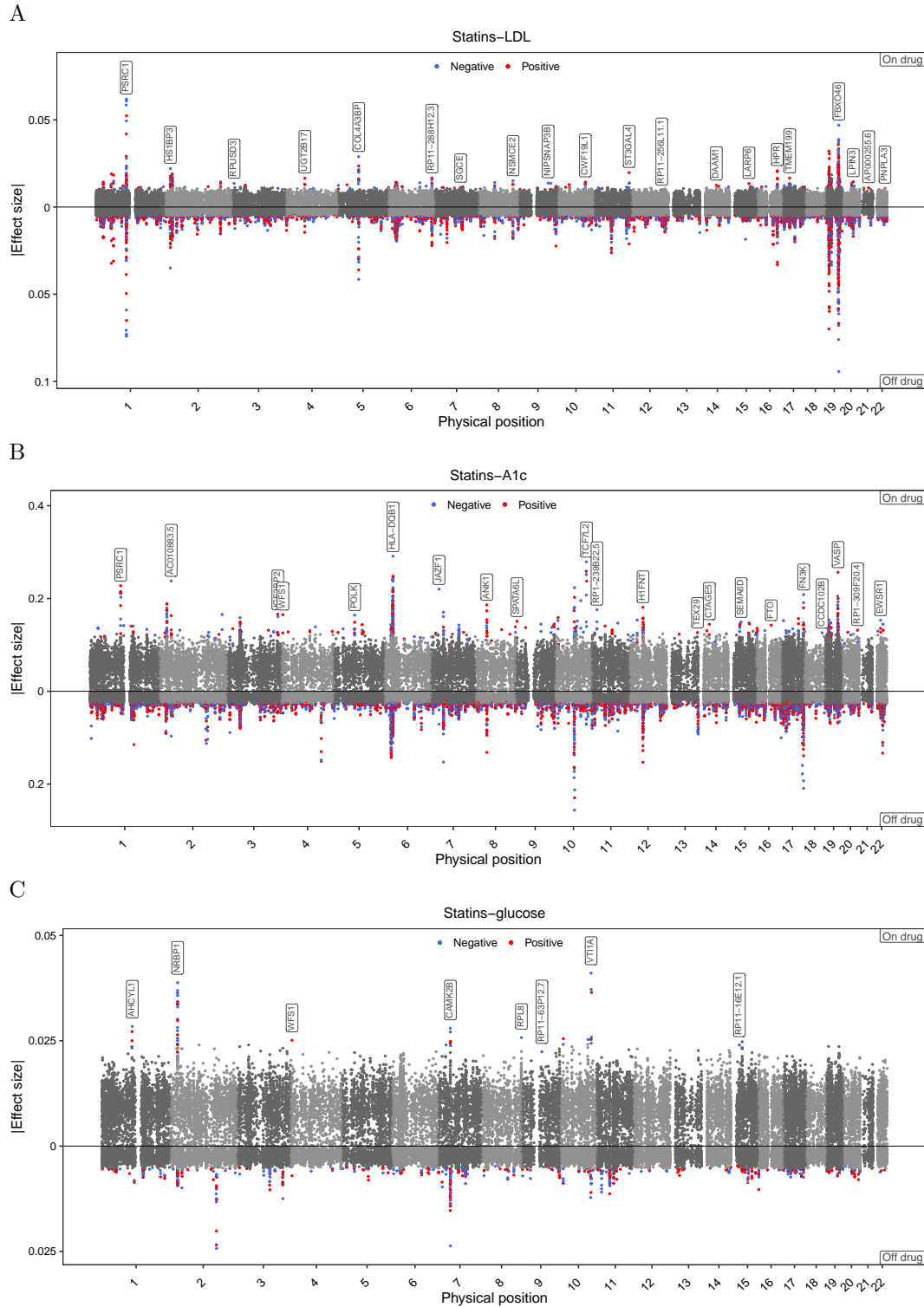


Figure S4. Manhattan plots of TWAS associations for LDL cholesterol, and A1c and blood glucose, obtained in statin users (top) and statin non-users (bottom); related to Figure 2. (A) LDL cholesterol. Each point represents a single gene, with physical position plotted on the x-axis and effect size plotted on the y-axis. The most extreme effect across tissues is shown for each gene. Significant associations are highlighted in blue (negative effects) and red (positive effects), and the strongest on-drug associations on each chromosome are labeled. (B) and (C) follow (A), but for A1c and blood glucose.

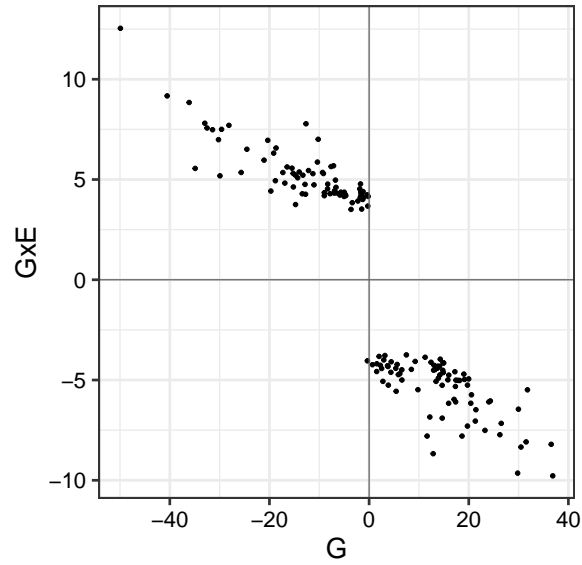


Figure S5. Z-scores for the main (G) and interaction (GxE) effects of genes whose interactions with statins were significantly associated with LDL cholesterol in TxEWAS; related to Figure 3. For each gene, we plot the estimates corresponding to the tissue with the strongest interaction p-value.

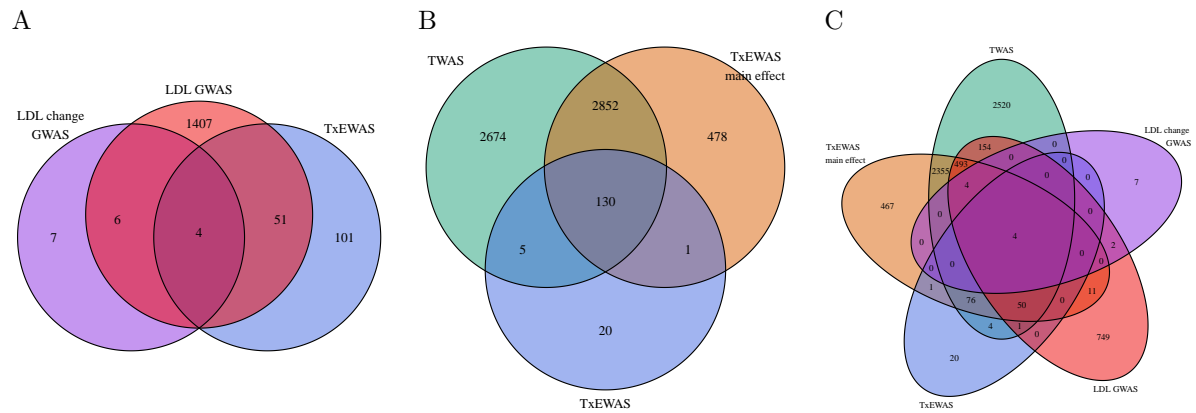


Figure S6. Overlap between genes identified or reported in the four following studies: (1) TxEWAS of statin interactions for LDL cholesterol (TxEWAS), (2) TWAS for LDL cholesterol (TWAS), (3) GWAS for LDL cholesterol change in response to statin therapy (LDL change GWAS), and (4) GWAS for LDL cholesterol (LDL GWAS); related to Figure 2. (A) Overlap between 1, 3 and 4. (B) Overlap between 1, 2, and main genetic effects from 1. (C) Overlap between 1, 2, 3, 4, and main genetic effects from 1.

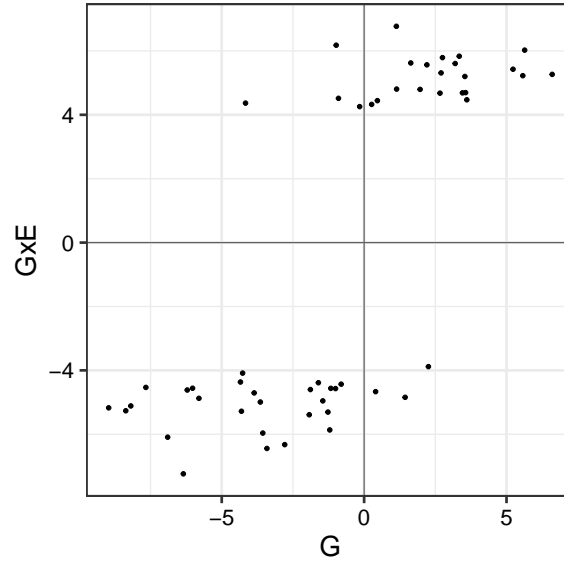


Figure S7. Z-scores for the main (G) and interaction (GxE) effects of genes whose interactions with statins were significantly associated with A1c in TxEWAS; related to Figure 3. For each gene, we plot the estimates corresponding to the tissue with the strongest interaction p-value.

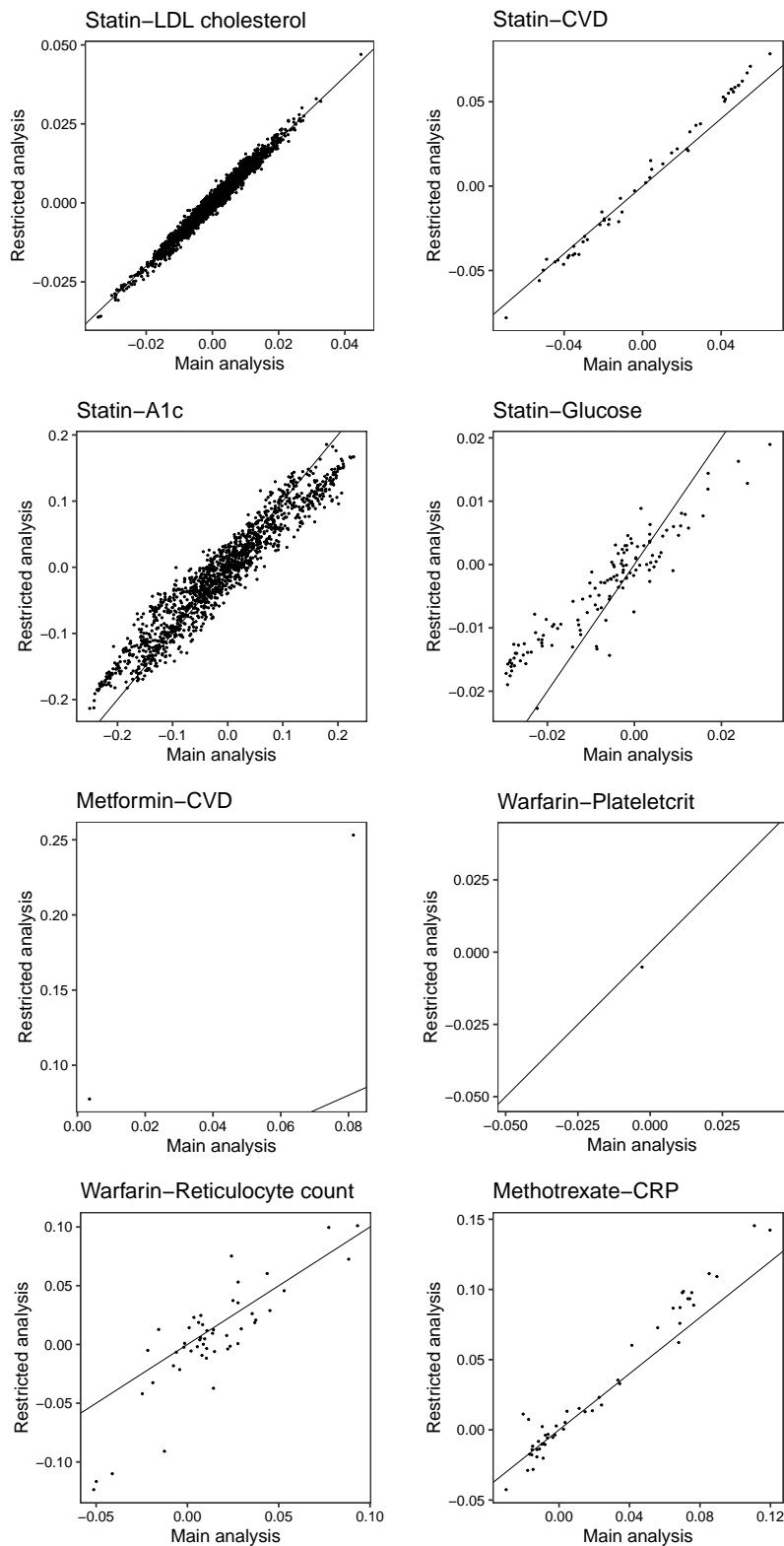


Figure S8. TxEWAS effect sizes of gene-drug interactions significantly associated with a phenotype either in the main analysis (using all users of a certain drug in the population studied) or the restricted analysis (using users of a certain drug who are non-users for the other drugs considered in the study); related to Figure 2. Effect sizes in all tested tissues are shown.

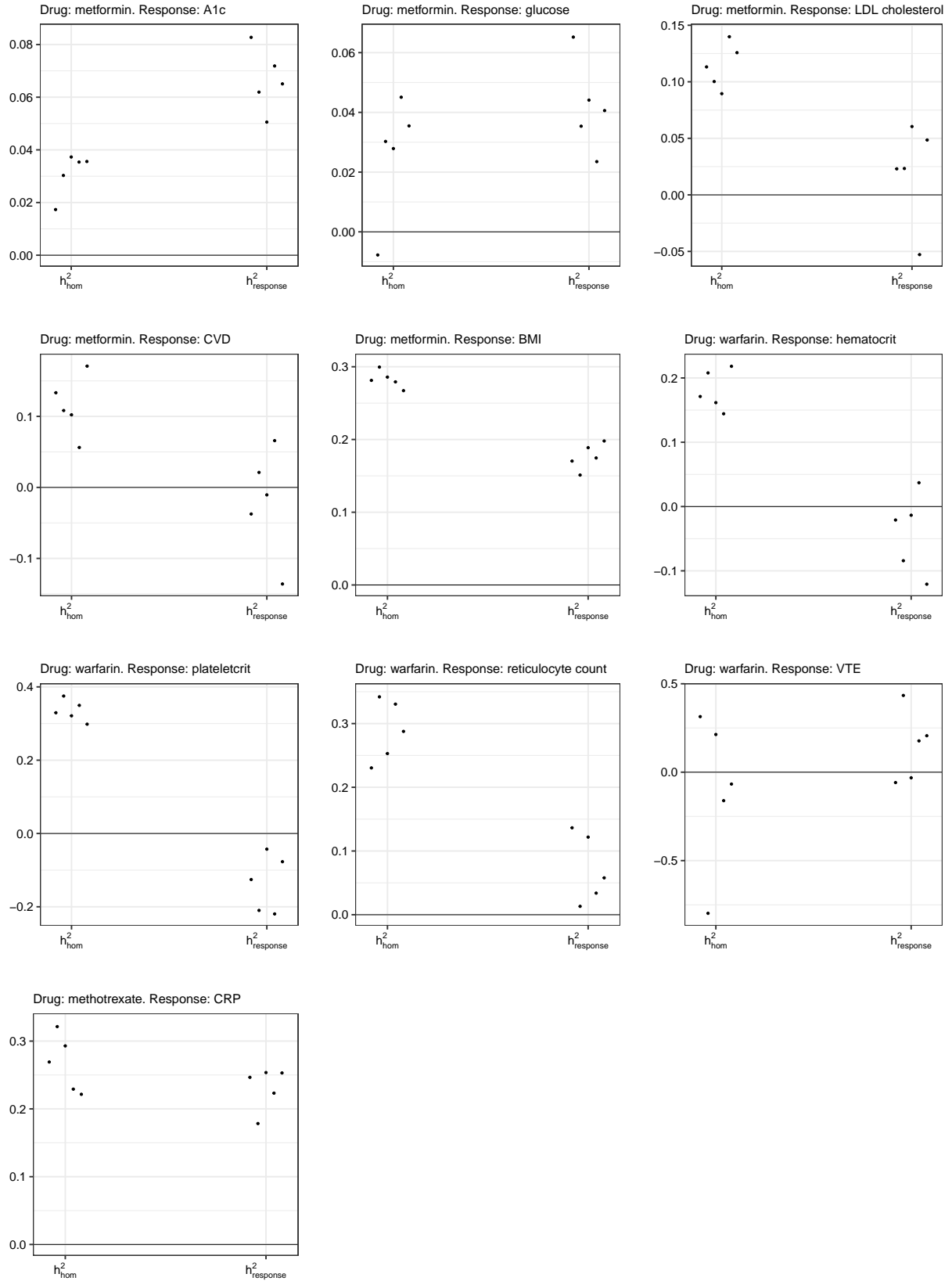


Figure S9. Estimation of drug-independent heritability ( $h^2_{\text{hom}}$ ), and heritability of drug response ( $h^2_{\text{response}}$ ) repeated five times with randomly resampled non-users; related to STAR Methods.

## 2 Supplemental Tables

Table S1. Drug-independent heritability ( $h^2_{\text{hom}}$ ), and heritability of drug response ( $h^2_{\text{response}}$ ) for a range of drug exposures and responses; related to Table 2.

Drug exposure	Response	$h^2_{\text{hom}}$	$h^2_{\text{response}}$	$h^2_{\text{response}}$ $p$ value
Statins	LDL cholesterol	0.208	0.0892	$1.13 \times 10^{-30}$
	CVD	0.086	0.0118	0.797
	A1c	0.285	0.1018	$1.79 \times 10^{-6}$
	Glucose	0.112	0.1114	$2.26 \times 10^{-4}$
	T2D	0.319	-0.0119	0.936
Metformin	A1c	0.035	0.0719	0.516
	Glucose	0.030	0.0354	0.907
	LDL cholesterol	0.113	0.0230	0.016
	CVD	0.108	0.0211	0.924
	BMI	0.281	0.1703	$2.51 \times 10^{-4}$
Warfarin	Hematocrit	0.171	-0.0209	0.991
	Plateletcrit	0.329	-0.1257	0.291
	Reticulocyte count	0.288	0.0579	0.627
	VTE	-0.067	0.2062	0.840
Methotrexate	CRP	0.269	0.2466	0.337

Table S2. Off-drug ( $h_{\text{off}}^2$ ) and on-drug ( $h_{\text{on}}^2$ ) heritability estimates for a range of drug exposures and responses; related to Table 2. Note that  $h_{\text{off}}^2$  and  $h_{\text{on}}^2$  are generally higher than  $h_{\text{hom}}^2$ , because they additionally capture genetic effects specific to on-drug and off-drug individuals, respectively.

Drug exposure	Response	$h_{\text{off}}^2$ (SE)	$h_{\text{on}}^2$ (SE)
Statins	LDL cholesterol	0.4125 (0.0080)	0.270 (0.034)
	CVD	0.1029 (0.0739)	0.075 (0.081)
	A1c	0.3170 (0.0075)	0.286 (0.034)
	Glucose	0.0924 (0.0068)	0.213 (0.033)
	T2D	0.2820 (0.4547)	0.119 (0.035)
Metformin	A1c	0.3040 (0.0568)	0.081 (0.147)
	Glucose	0.0758 (0.0302)	0.057 (0.106)
	LDL cholesterol	0.2294 (0.0317)	0.114 (0.075)
	CVD	0.1975 (0.3253)	0.067 (0.137)
	BMI	0.3073 (0.0300)	0.513 (0.073)
Warfarin	Hematocrit	0.2647 (0.0296)	0.153 (0.187)
	Plateletcrit	0.3936 (0.0231)	0.180 (0.112)
	Reticulocyte count	0.3385 (0.0209)	0.337 (0.138)
	VTE	0.1386 (0.5809)	0.185 (0.604)
Methotrexate	CRP	0.3457 (0.0202)	0.549 (0.248)

Table S3. Heritability of LDL cholesterol, A1c and glucose in individuals on statin-metformin drug combinations, estimated by the (additive) GCTA model; related to Table 2. A small number of metformin users who do not take statins (1,583) has not allowed for reliable estimation in this group.

		LDL cholesterol		A1c		Glucose	
		Statins		Statins		Statins	
		Non-users	Users	Non-users	Users	Non-users	Users
Metformin	Non-users	0.534 (0.074)	0.335 (0.077)	0.401 (0.085)	0.391 (0.082)	0.121 (0.087)	0.025 (0.092)
	Users	0.000 (0.281)	0.244 (0.074)	0.000 (0.347)	0.101 (0.077)	0.860 (0.397)	0.088 (0.090)

Table S4. Variance decomposition with GxEMM for a range of drug exposures and responses; related to Table 2.

Drug exposure	Response	$\sigma_{\text{hom}}^2$ (SE)	$v_{0(\text{off})}$ (SE)	$v_{1(\text{on})}$ (SE)	$w_{0(\text{off})}$ (SE)	$w_{1(\text{on})}$ (SE)
Statins	LDL cholesterol	0.2077 (0.0090)	0.1414 (0.0110)	-0.0483 (0.0216)	0.4973 (0.0068)	0.4528 (0.0214)
	CVD	0.0860 (0.0400)	-0.0049 (0.0501)	0.0315 (0.1101)	0.7637 (0.2682)	1.4621 (0.4331)
	A1c	0.2849 (0.0132)	-0.0840 (0.0138)	0.2989 (0.0698)	0.4328 (0.0049)	1.4629 (0.0698)
	Glucose	0.1116 (0.0131)	-0.0450 (0.0137)	0.3361 (0.0695)	0.6600 (0.0052)	1.6615 (0.0694)
	T2D	0.3187 (0.0481)	-0.0825 (0.0647)	0.0473 (0.0983)	0.2676 (0.7135)	2.7246 (0.3624)
Metformin	A1c	0.0354 (0.0328)	0.0398 (0.0352)	0.0394 (0.1348)	0.1720 (0.0144)	0.8505 (0.1368)
	Glucose	0.0303 (0.0334)	-0.0054 (0.0344)	0.0886 (0.2220)	0.3037 (0.0113)	1.9657 (0.2222)
	LDL cholesterol	0.1132 (0.0233)	0.0778 (0.0337)	-0.0513 (0.0436)	0.6415 (0.0264)	0.4803 (0.0412)
	CVD	0.1083 (0.0929)	0.0518 (0.1310)	-0.0072 (0.1826)	0.6507 (1.1650)	1.4190 (1.2552)
	BMI	0.2813 (0.0292)	-0.0618 (0.0350)	0.2706 (0.0828)	0.4948 (0.0216)	0.5222 (0.0782)
Warfarin	Hematocrit	0.1712 (0.0427)	-0.0023 (0.0459)	-0.0241 (0.1808)	0.4694 (0.0190)	0.8145 (0.1807)
	Plateletcrit	0.3295 (0.0369)	0.0108 (0.0409)	-0.1570 (0.1009)	0.5243 (0.0199)	0.7850 (0.1082)
	Reticulocyte count	0.2877 (0.0372)	0.0400 (0.0417)	0.0389 (0.1369)	0.6404 (0.0203)	0.6433 (0.1338)
	VTE	-0.0671 (0.3474)	0.1863 (0.4042)	0.4819 (1.3094)	0.7404 (1.4170)	1.8327 (4.2795)
Methotrexate	CRP	0.2692 (0.0536)	0.0550 (0.0563)	0.2986 (0.2573)	0.6135 (0.0189)	0.4670 (0.2559)



Table S6. Enrichment of gene-statin interactions for LDL cholesterol in pathway-based gene sets at 1% significance level; related to Figure 2.

Pathway	Source	Genes	<i>p</i> value
Herpes simplex virus 1 infection	KEGG	ZNF627, ZNF235, ZNF234, ZNF233, ZNF222, TYK2, ZNF225, ZNF700, NECTIN2, ZNF433, ZNF284, ZNF45, ZNF223, ZNF224, NXF1, ZNF226, ZNF227, ZNF229, ZNF589, ZNF440, ZNF441, ZNF155, ZNF112	3.01e-12
Cholesterol metabolism	KEGG	PCSK9, LPL, ANGPTL8, APOE, APOC1	5.76e-05
Generic Transcription Pathway	Reactome	ZNF627, ZNF235, ZNF234, ZNF233, ZNF45, SMARCA4, APOE, ZNF700, ZNF433, ZNF222, ZNF223, ZNF224, ZNF225, ZNF226, ZNF227, ZNF589, GATAD2A, ZNF440, ZNF441, ZNF155, PPP1R13L, ZNF112	5.78e-05
Plasma lipoprotein assembly, remodeling, and clearance	Reactome	PCSK9, LPL, APOE, ANGPTL8, APOC1	1.59e-04
RNA Polymerase II Transcription	Reactome	ZNF627, ZNF235, ZNF234, ZNF233, ZNF45, SMARCA4, APOE, ZNF700, ZNF433, ZNF222, ZNF223, ZNF224, ZNF225, ZNF226, ZNF227, ZNF589, GATAD2A, ZNF440, ZNF441, ZNF155, PPP1R13L, ZNF112	2.81e-04
Omega-3 fatty acid metabolism	EHMN	FADS1, FADS3, FADS2	2.88e-04
Gene expression (Transcription)	Reactome	ZNF627, ZNF235, ZNF234, ZNF233, ZNF45, SMARCA4, APOE, ZNF700, DNMT1, ZNF433, ZNF222, ZNF223, ZNF224, ZNF225, ZNF226, ZNF227, ZNF589, PPP1R13L, ZNF440, ZNF441, ZNF155, GATAD2A, ZNF112	4.64e-04
Nectin/Necl trans heterodimerization	Reactome	NECTIN2, PVR	4.66e-04
Alpha Linolenic Acid and Linoleic Acid Metabolism	SMPDB	FADS1, FADS2	7.72e-04
Metabolic pathway of LDL, HDL and TG, including diseases	Wikipathways	LPL, PCSK9	1.15e-03
Plasma lipoprotein remodeling	Reactome	LPL, APOE, ANGPTL8	1.21e-03
Linoleate metabolism	EHMN	FADS1, CYP2C8, FADS3, FADS2	1.33e-03
Omega-6 fatty acid metabolism	EHMN	FADS1, FADS3, FADS2	1.54e-03
Statin inhibition of cholesterol production	Wikipathways	LPL, APOE, APOC1	1.54e-03
Linoleic acid (LA) metabolism	Reactome	FADS1, FADS2	1.60e-03
Plasma lipoprotein clearance	Reactome	PCSK9, APOE, APOC1	2.12e-03
Chylomicron remodeling	Reactome	LPL, APOE	2.12e-03
oleate biosynthesis	HumanCyc	FADS1, FADS2	2.12e-03
eicosapentaenoate biosynthesis	HumanCyc	FADS1, FADS2	3.37e-03
Omega-9 FA synthesis	Wikipathways	FADS1, FADS2	4.10e-03
alpha-linolenic acid (ALA) metabolism	Reactome	FADS1, FADS2	4.89e-03
alpha-linolenic (omega3) and linoleic (omega6) acid metabolism	Reactome	FADS1, FADS2	4.89e-03
Assembly of active LPL and LIPC lipase complexes	Reactome	LPL, ANGPTL8	4.89e-03
Omega-3-Omega-6 FA synthesis	Wikipathways	FADS1, FADS2	5.75e-03
LKB1 signaling events	PID	MARK4, SIK1, CDC37	6.12e-03
Plasma lipoprotein assembly	Reactome	APOE, APOC1	8.69e-03
Deregulated CDK5 triggers multiple neurodegenerative pathways in Alzheimer's disease models	Reactome	CAST, CDC25A	9.79e-03
Neurodegenerative Diseases	Reactome	CAST, CDC25A	9.79e-03

Table S7. Enrichment of replicated and not reported in LDL cholesterol GWAS gene-statin interactions for LDL cholesterol in pathway-based gene sets at 1% significance level; related to Figure 2.

Pathway	Source	Genes	<i>p</i> value
Herpes simplex virus 1 infection - Homo sapiens (human)	KEGG	ZNF224, ZNF226, ZNF227, ZNF229, ZNF235, NECTIN2, ZNF284, ZNF112	6.63e-08
Nectin/Necl trans heterodimerization	Reactome	NECTIN2, PVR	1.24e-05
Plasma lipoprotein assembly	Reactome	APOE, APOC1	2.45e-04
Statin inhibition of cholesterol production	Wikipathways	APOE, APOC1	6.58e-04
Adherens junctions interactions	Reactome	NECTIN2, PVR	6.58e-04
Nectin adhesion pathway	PID	NECTIN2, PVR	7.64e-04
Plasma lipoprotein clearance	Reactome	APOE, APOC1	8.20e-04
NR1H3 & NR1H2 regulate gene expression linked to cholesterol transport and efflux	Reactome	APOE, APOC1	1.19e-03
NR1H2 and NR1H3-mediated signaling	Reactome	APOE, APOC1	1.89e-03
Cholesterol metabolism - Homo sapiens (human)	KEGG	APOE, APOC1	2.15e-03
Generic Transcription Pathway	Reactome	APOE, ZNF224, ZNF226, ZNF227, ZNF235, ZNF112	2.32e-03
Apoptosis-related network due to altered Notch3 in ovarian cancer	Wikipathways	APOE, BCL3	2.53e-03
Cell-cell junction organization	Reactome	NECTIN2, PVR	2.62e-03
Plasma lipoprotein assembly, remodeling, and clearance	Reactome	APOE, APOC1	3.25e-03
RNA Polymerase II Transcription	Reactome	APOE, ZNF224, ZNF226, ZNF227, ZNF235, ZNF112	4.03e-03
Cell junction organization	Reactome	NECTIN2, PVR	5.38e-03
Gene expression (Transcription)	Reactome	APOE, ZNF224, ZNF226, ZNF227, ZNF235, ZNF112	6.75e-03
C-type lectin receptor signaling pathway - Homo sapiens (human)	KEGG	RELB, BCL3	9.22e-03

Table S8. Simulation of polygenic prediction in individuals on and off a treatment; related to Table 3.

PGS	Prediction accuracy ( $R^2$ )			
	Scenario 1		Scenario 2	
	On drug	Off drug	On drug	Off drug
on-drug-PGS	0.0881	0.2654	0.3613	0.2091
off-drug-PGS	0.0940	0.2838	0.2548	0.2955
all-PGS	0.0942	0.2844	0.3379	0.2699

Table S9. Prediction accuracy of a PGS as a function of training population (rows) and test population (columns); related to Table 3. In order, training populations/rows are: drug users; non-users, subsampled to match the number of drug users; a similarly subsampled 50:50 mixture of users and non-users without adjustment for treatment as a covariate; the same 50:50 mixture with adjustment; and a 50:50 mixture of users and subsampled non-users pooled together, with adjustment. The last two rows report prediction accuracy of combinations of above PGSs tested jointly (Section 3.4).

PGS	Prediction accuracy (Incremental $R^2$ [%](SE))							
	Statins				Metformin			
	LDL cholesterol		A1c		LDL cholesterol		BMI	
	On drug	Off drug	On drug	Off drug	On drug	Off drug	On drug	Off drug
on-drug-PGS	7.18 (0.30)	12.60 (0.36)	3.36 (0.23)	2.32 (0.18)	1.32 (0.37)	3.24 (0.54)	0.919 (0.286)	0.0040 (0.0592)
off-drug-PGS	7.98 (0.32)	14.87 (0.39)	2.56 (0.20)	5.79 (0.28)	2.75 (0.51)	5.43 (0.67)	0.041 (0.080)	0.0077 (0.0636)
agnostic-PGS	5.86 (0.29)	10.49 (0.36)	2.60 (0.20)	3.75 (0.23)	2.25 (0.44)	5.00 (0.66)	0.255 (0.164)	0.0931 (0.1078)
adjusted-PGS	7.67 (0.32)	13.59 (0.38)	2.80 (0.21)	3.75 (0.22)	2.14 (0.45)	5.24 (0.67)	0.193 (0.141)	-0.0205 (0.0370)
adjusted-all-PGS	8.62 (0.32)	15.66 (0.42)	4.70 (0.26)	5.62 (0.25)	3.01 (0.53)	6.63 (0.74)	0.212 (0.148)	0.0477 (0.0843)
on-drug-PGS + off-drug-PGS	8.15 (0.34)	14.93 (0.40)	4.12 (0.24)	6.02 (0.28)	2.74 (0.51)	5.42 (0.66)	0.959 (0.299)	0.0120 (0.0851)
adjusted-all-PGS + on-drug-PGS + off-drug-PGS	8.65 (0.33)	15.82 (0.40)	4.72 (0.26)	6.82 (0.30)	3.12 (0.55)	6.70 (0.79)	0.950 (0.305)	0.0341 (0.1029)

Table S10. Heritability of LDL cholesterol, A1c and glucose estimated with the additive GCTA model with adjustment for statin or metformin use, or without adjustment; related to Table 2.

Drug added to covariates	$h^2_{\text{GCTA}}$ (SE)		
	LDL cholesterol	A1c	Glucose
None	0.2268 (0.0054)	0.2837 (0.0055)	0.0938 (0.0055)
Statins	0.3780 (0.0055)	0.2767 (0.0055)	0.0892 (0.0055)
Metformin	0.2115 (0.0179)	0.1521 (0.0176)	0.0476 (0.0167)

## 3 Supplemental Note

### 3.1 Variance decomposition analysis with GxEMM

#### 3.1.1 The GxEMM model

We quantify heritable effects on drug response using GxEMM, a linear mixed model for genome-wide gene-environment interactions [S1]. GxEMM quantifies the heritability contributed by genome-wide additive effects and genome-wide GxE effects. The general GxEMM model is:

$$\begin{aligned} y &= X\alpha + G\beta + (G * Z)\gamma + (I * Z)\epsilon \\ \beta_l &\overset{\text{iid}}{\sim} \mathcal{N}\left(0, \frac{1}{L}\sigma_{\text{hom}}^2\right) \\ \gamma_{(l,i)} &\overset{\text{iid}}{\sim} \mathcal{N}\left(0, \frac{1}{L}V\right) \\ \epsilon_i &\overset{\text{iid}}{\sim} \mathcal{N}(0, W) \end{aligned}$$

In this model, the known data are:

- $y$  is the quantitative phenotype
- $X$  are covariates with fixed effects  $\alpha$ , like age or sex.
- $G$  is a centered and scaled matrix of genome-wide genotypes
- $Z$  is matrix of context features. In our study,  $Z_i = (0, 1)$  if individual  $i$  is treated, and  $Z_i = (1, 0)$  if individual  $i$  is untreated
- $*$  is the column-wise Khatri-Rao product, which forms the interaction between two design matrices. For example, each column of  $G * Z$  is of the form  $G_{\cdot j} \circ Z_{\cdot k}$ , where  $\circ$  takes the element-wise product between SNP  $j$  and context feature  $k$

The random effects and their corresponding variance components are:

- $\beta_l$  is the effect of SNP  $l$  that is shared across contexts.  $\sigma_{\text{hom}}^2$  is the additive genetic variance—i.e., the size of  $\sum_l \beta_l$
- $\gamma_{(lk)}$  is the effect of SNP  $l$  that is specific to context  $k$ .  $v_k := V_{kk}$  is the genetic variance specific to context  $k$ —i.e., the size of  $\sum_l \gamma_{(lk)}$
- $\epsilon_{(ik)}$  is the noise for individual  $i$  from context  $k$ .  $w_k := W_{kk}$  is the noise variance in context  $k$ .

Finally, the cross-context covariance terms are:

- $v_{12} := V_{12}$  is the genetic covariance between contexts. Because  $Z$  is binary in our setting, this term be ignored WLOG—it can be folded in with  $\sigma_{\text{hom}}^2$  [S1]
- $w_{12} := W_{12}$  is the noise covariance between contexts 1 and 2. In our setting with binary  $Z$ , this term cannot be identified—an individual either has noise  $\epsilon_1$  or  $\epsilon_2$ , but we cannot observe the covariance between these terms in cross-sectional data.
- **Comparing to main text parameters.** In the main text, we use simpler notation to simplify the presentation. Specifically,  $v_0$  and  $v_1$  in the main text correspond to  $V_{11}$  and  $V_{22}$  here, respectively (and likewise for  $w_0$ , and  $w_1$ ).  $W_{12}$  appears as  $w_{01}$ .  $V_{12}$  does not appear in the main text.

While neither  $v_{12}$  nor  $w_{12}$  can be identified in our cross-sectional data, they are different in an important way. Specifically,  $v_{12}$  can be assumed 0 WLOG, because it is already captured in  $\sigma_{\text{hom}}^2$ . However,  $w_{12}$  cannot be assumed to be zero—we simply have no data to learn about this parameter.

To unpack the model, imagine studying genetic effects on LDL cholesterol across statin users and non-users. A SNP  $s$  that equally increases LDL cholesterol in both groups has a homogeneous effect ( $\beta_s > 0$ ) but has no drug-specific effects ( $\gamma_{s1} = \gamma_{s2} = 0$ ), so  $s$  contributes to  $\sigma_{\text{hom}}^2$  but not  $v_1$  or  $v_2$ . Conversely, a SNP  $s'$  that increases LDL cholesterol only in statin users has  $\beta_{s'} = 0$  and  $\gamma_{s'2} > \gamma_{s'1} = 0$ , so  $s'$  contributes to  $v_2$  but not  $\sigma_{\text{hom}}^2$  or  $v_1$ . Finally,  $w_2 > w_1$  means that statin users have higher non-genetic LDL cholesterol variance.

In various special cases, GxEMM is similar or identical to other methods that fit genome-wide GxE heritability [S2, S3, S4]. For example, the method from [S3] applies to categorical environments and continuous phenotypes and, thus, would apply to our analyses of quantitative phenotypes (such as LDL cholesterol or A1c) but would not apply to our analyses of binary disorders (such as T2D or CVD). Finally, GxEMM reduces to the ordinary additive heritability model when  $V = 0$  and  $w_1 = w_2$ , i.e., when neither genetic nor nongenetic variance depends on the environment.

### 3.1.2 Using GxEMM to estimate treatment response heritability

If we had measures of a phenotype before and after a treatment, we could directly calculate the change in phenotype,  $\Delta y$ , and then estimate its heritability using standard heritability estimation methods. This would be ideal, as the change in phenotype captured in  $\Delta y$  cancels out the contribution of all covariates and unmodelled noise that do not depend on treatment status.

In contrast, we are interested in the setting where we only measure each individual's phenotype before or after treatment. This is motivated by large cross-sectional biobank data like UK Biobank, where most individuals are only observed at one time point. Here, we show how to approximate the heritability of  $\Delta y$  in this setting using GxEMM.

How is this possible if we never observe  $\Delta y$ ? Imagine we only see individual  $i$  pre-treatment ( $E_i = 0$ ), but that we see their relative  $j$  post-treatment ( $E_j = 1$ ). Intuitively, we can use individual  $j$ 's post-treatment phenotype to proxy for individual  $i$ 's post-treatment phenotype. More specifically, individual  $j$  will be a proxy for the genetic part of individual  $i$ . Intuitively, individual  $j$  cannot inform the nongenetic part of individual  $i$ 's phenotype; mathematically, this is equivalent to our above observation that  $w_{12}$  is not identified.

To declutter notation, consider a single individual's phenotype  $y$  and genotype vector  $g$ . Let  $\gamma_1$  indicate the effects of all  $S$  SNPs in untreated individuals ( $E = 0$ ), and let  $\gamma_2$  indicate the effects of the SNPs in treated individuals ( $E = 1$ ). Informally define  $\Delta y$  as  $y(E = 1) - y(E = 0)$ , i.e., the phenotype change after an individual is treated.  $\Delta y$  is unobserved because we only observe either the treated or untreated state. Our goal is to estimate the heritability of this unobserved phenotype using GxEMM. Under the GxEMM model defined above, we have:

$$\begin{aligned} \Delta y &= y(E = 1) - y(E = 0) \\ &= (g\beta + g\gamma_2 + \epsilon_2) - (g\beta + g\gamma_1 + \epsilon_1) \\ &= g(\gamma_2 - \gamma_1) + (\epsilon_2 - \epsilon_1) \implies \\ \mathbb{V}(\Delta y) &= \text{tr}(g^T g \mathbb{V}(\gamma_2 - \gamma_1)) + \mathbb{V}(\epsilon_2 - \epsilon_1) \\ &= \text{tr}\left(g^T g \frac{1}{L} I_L (v_{11} + v_{22})\right) + (w_{11} + w_{22} - 2w_{12}) \\ &= (v_{11} + v_{22}) + (w_{11} + w_{22} - 2w_{12}) \end{aligned}$$

GxEMM can estimate all of these parameters—except for  $w_{12}$ . Intuitively, it captures the covariance in effect sizes for unmodelled risk factors between treated/untreated states. We can safely assume that  $w_{12}$  is nonnegative: Otherwise, the majority of unmodelled nongenetic risk factors would have opposite effects in the treated/untreated contexts. For example, if smoking status was the only unmodelled risk factor for LDL cholesterol, then  $w_{12} < 0$  implies smoking becomes protective after statin administration. We emphasize that this is a biological assumption, not a mathematical assumption.

Therefore, we can estimate the heritability of treatment response by:

$$\begin{aligned}
h_{\text{response}}^2 &:= h^2(\Delta y) \\
&= \frac{v_{11} + v_{22}}{v_{11} + v_{22} + w_{11} + w_{22} - 2w_{12}} \\
&\geq \frac{v_{11} + v_{22}}{v_{11} + v_{22} + w_{11} + w_{22}}
\end{aligned}$$

We call this “conservative” in the main text to emphasize that the heritability is underestimated when  $w_{12} > 0$ , and in this sense the inequality is mathematically conservative. But, again, we will overestimate  $h^2$  in the unlikely case where  $w_{12} < 0$ .

Finally, we note that these calculations ignore endogeneity in treatment status. This is hiding in our informal definition of  $\Delta y$ , which imagines that we observe an individual in  $E = 0$  or  $E = 1$  state at random. However, when the treatment is prescribed based on  $y$  itself, we are ignoring a subtle form of dependence between  $E$  and  $G$  (that is more pernicious than mere G-E correlation, which does not generally cause bias in GxEMM [S1]). This is worth theoretically solving in future work; here, we use simulations to evaluate the implications of this potential bias.

### 3.1.3 Negative estimates of drug-specific genetic variance

Some of the drug-specific genetic variance estimates obtained in this study are negative (Table S4). We demonstrate in simulation that such observations are expected when a drug has a buffering effect.

We simulated 10,000 non-users and 5,000 users of a hypothetical drug. A phenotype of each non-user was simulated as a sum of minor-allele effects at 1000 SNPs plus a noise term drawn from a normal distribution with a zero mean and a variance selected to obtain a particular heritability of the phenotype ( $h^2$ ). Each of the SNPs was drawn independently from a binomial distribution  $B(2, p)$  with  $p$  representing the minor allele frequency, which was drawn uniformly from a range between 0.2 and 0.5. SNP effects were drawn from a normal distribution with zero mean and variance  $\sigma_g^2 = h^2/1000$ . Users’ phenotypes were generated similarly, with the only difference being that the effects of a randomly selected half of the SNPs were shrunk twofold, representing a buffering effect of the drug.

We find that GxEMM produces a negative value of drug-specific genetic variance ( $v_1$ ) on average across simulation replicates (Figure S3). We note that all heritability parameters ( $h_{\text{off}}^2$ ,  $h_{\text{on}}^2$ , and  $h_{\text{response}}^2$ ) remain non-negative, as expected. This is consistent with our empirical results, where  $v_1$  may be negative but no heritability estimate is significantly less than zero (Tables S1 and S2).

We note that although buffering is a plausible cause for negative  $v_1$  in the context of our work, the above simulation does not prove that this buffering model is the only possible model to explain negative  $v_1$ . More generally, parameters  $v_0$  and  $v_1$  should be interpreted as offsets from  $h_{\text{hom}}^2$ , and thus can be negative when one group has higher genetic variance than another. That is, the total genetic variance in the on-drug group is  $h_{\text{hom}}^2 + v_1$ , and this should be nonnegative; but if  $h_{\text{hom}}^2$  is larger than the genetic variance in this group, then  $v_1$  should be negative.  $v_0$  and  $v_1$  are internal model parameters that are a means to the directly interpretable heritability parameters that we focus on in the main text,  $h_{\text{off}}^2$ ,  $h_{\text{on}}^2$ , and  $h_{\text{response}}^2$ .

### 3.1.4 Dependence of heritability estimates on covariates

In our analysis, estimates of  $h_{\text{hom}}^2$  for a given outcome vary depending on which drug we test for interaction (Table S1). This is because we always adjust for the main effect of a specific drug being tested. This is important to avoid false positive gene-drug interactions, but can substantially affect the phenotype variance components because drug effects can be large.

This dependence on the choice of covariates is common to all heritability estimation methods and has been discussed before [S5]. To illustrate this point, we show that the ordinary additive estimates of heritability calculated with GCTA [S6] exhibit similar behavior to the corresponding  $h_{\text{hom}}^2$  estimates (Table S10).

## 3.2 TxEWAS for detection of gene-drug interactions

### 3.2.1 The TxEWAS model

To identify specific genes involved in drug response from cross-sectional data, we use a newly developed statistical framework, TxEWAS, which extends the transcriptome-wide association study (TWAS [S7, S8]) framework. TxEWAS addresses shortcomings of SNP-level GxE studies—it improves power by reducing the number of tests, and interpretability by directly suggesting possible causal genes.

The TxEWAS framework involves two major steps: First, gene expression levels of each gene are genetically imputed using a reference dataset. Second, the interaction effect between imputed gene expression and the drug is tested.

In case where a response  $y_i$  is continuous, the interaction effect ( $\beta_6$ ) is tested in the linear regression model:

$$y_i \sim \mathcal{N} \left( \beta_0 + \sum_j \beta_{1j} c_{i,j} + \sum_j \beta_{2j} e_i c_{i,j} + \sum_j \beta_{3j} g_i c_{i,j} + \beta_4 g_i + \beta_5 e_i + \beta_6 g_i e_i, \sigma^2 \right),$$

where  $e_i$  and  $g_i$  are drug use indicator and imputed expression of some gene for individual  $i$ , respectively; and  $c_{i,j}$  is an element of a matrix of covariates  $\mathbf{C}$ .  $\beta_4$  and  $\beta_5$  are what we call “main” or “additive” effects of a gene and drug, respectively.

In case where the response is binary, the interaction effect is tested in the logistic regression model:

$$y_i \sim \text{Bernoulli} \left( \text{logit}^{-1} \left( \beta_0 + \sum_j \beta_{1j} c_{i,j} + \sum_j \beta_{2j} e_i c_{i,j} + \sum_j \beta_{3j} g_i c_{i,j} + \beta_4 g_i + \beta_5 e_i + \beta_6 g_i e_i \right) \right).$$

The variance of the effect size estimates is estimated with the robust sandwich variance estimator (SVE). In the linear regression-based test, their role is to control for both heteroscedasticity [S9] and misspecification of the functional form of the environmental factor [S10, S11]. In the logistic regression-based test, they are meant to account for the latter. The bias caused by the violation of the homoscedasticity assumption of the linear regression model is a specifically important concern in GxE studies. We therefore perform extensive simulations and permutation analyses to test that the TxEWAS model is calibrated (Section 3.2.2).

We note that even though in this work we use TxEWAS to detect gene-drug interactions, any environment can be tested with this method.

### 3.2.2 TxEWAS performance in simulations

In the presence of environment-conditional heteroscedasticity, testing multiple genetic variants for interaction with the environmental factor in a simple linear regression model results in an inflated or deflated false positive rate (FPR), depending on the relation between group size and phenotypic variation [S9]. We performed a simulation to assess the size of this bias in a dataset of the size and characteristics of the UK Biobank (Figure S1A).

In the simulation, we considered a binary environmental variable that divided observations into two groups of sizes  $n_1$  and  $n_2$ , and phenotype variances  $\sigma_1^2$  and  $\sigma_2^2$ . We simulated the phenotype as a Gaussian random variable with the corresponding group variances, but with no mean effects. The genotype was drawn from a binomial distribution with the same probability 0.4 of success for both groups. We fitted to this data GxE models that included the genotype, the environmental factor and the product of those two as covariates. For every selected value of the ratio  $\sigma_2^2/\sigma_1^2$ , we ran 5,000 such simulations, and calculated the FPR for the GxE effect as the proportion of simulations where the nominal  $p$  value for this effect was less than 0.05.

Group sizes used in the simulation were chosen based on the number of statin users in the UK Biobank ( $n_1 = 285,822$  and  $n_2 = 56,132$ ). Examples of  $\sigma_2^2/\sigma_1^2$  values that we encountered in the UK Biobank when stratifying individuals by statin use were: 0.68 for LDL cholesterol, 1.96 for blood glucose, or 3.00 for A1c.

The simulation shows that if the smaller (larger) group is characterized by the larger (smaller) variance of the response, the FPR for the GxE model fitted with ordinary least-squares (OLS) is inflated (deflated).



Within a realistic range of parameter values, the FPR can reach zero or increase threefold (Figure S1A). On the other hand, if the groups have equal sizes, the model is well calibrated. The bias can be controlled by using robust standard errors estimated with the sandwich variance estimator (SVE). This approach gives virtually the same results as the double generalized linear model (DGLM), which correctly models the phenotypic variance as a function of covariates, and is more computationally efficient than the latter.

Taking advantage of those facts, TxEWAS performs a linear regression-based interaction test and controls for heteroskedasticity with the SVE.

To investigate the type I error rate for TxEWAS in real data, we performed a permutation analysis where we randomly shuffled imputed expression of 4,516 liver genes across subjects. We selected statin for drug exposure, and LDL cholesterol and blood glucose for responses to examine both deflation and inflation biases ( $\sigma_2^2/\sigma_1^2 = 0.68$  and  $\sigma_2^2/\sigma_1^2 = 1.96$ , respectively). The analysis demonstrates that the TxEWAS model is well calibrated, even though  $p$  values estimated with the simple linear regression-based interaction test are heavily deflated or inflated, depending on the examined response (Figure S1B).

### 3.2.3 Combinations of treatments

Patients are often on multiple drugs simultaneously, for example, in the cohort studied in this work, out of the 8,606 individuals who reported taking metformin 6,946 also reported taking statins. This makes accompanying treatments an important potential confounder in our analyses. To test their impact on GxE, we repeated TxEWAS for each drug excluding individuals on the other drugs we consider—e.g., in the TxEWAS for statins, we excluded individuals taking metformin, warfarin, or methotrexate. We observe that the original results remain largely unaffected (Figure S8). For example, the statins-LDL analysis identified 127 interaction genes, from which 113 were among the 156 interaction genes found in the original analysis. Of those 127 genes, 126 could be studied in the replication cohort, and 35 replicated at hFDR < 10%. The remaining genes were enriched for low  $p$  values < 0.1 (binomial test=0.002).

## 3.3 Endogeneity bias

Like all existing gene-environment interaction models, GxEMM and TxEWAS are susceptible to endogeneity bias. In practice, drugs are not administered at random. When the causes of drug prescription are intertwined with causal effects on the focal phenotype, this is called endogeneity. In general, endogeneity can induce complex biases in statistical analyses.

A particularly relevant example to our analysis is when a drug is prescribed to lower a phenotype that exceeds a certain level. Statin therapy for high LDL cholesterol is such an example. Below we simulate two different effects that such a therapy could have in the population (first column in Figure S2): 1) the drug lowers the phenotype of every treated individual by the same amount, and 2) the drug is administered at a dose that achieves the same target level of the phenotype in all treated individuals. Modeling both simulated phenotypes with the GxE model yields GxE effects which are starkly negatively correlated with additive effects (second column in Figure S2), even though the phenotypes were generated in the absence of gene-drug interactions. We further show that the heritability of the change of the second phenotype (we selected one for simplicity) is substantial.

These simulation results are consistent with our empirical results for statins and LDL cholesterol. Indeed, endogeneity bias is surely present in our analyses and affects their results. However, to verify that our approach has ability to discover true gene-drug interactions, we replicated our gene-statin interaction effects on LDL cholesterol in a pharmacogenomic study. This study evades endogeneity bias by examining statin-induced LDL cholesterol change and adjusting for statin dose and other carefully selected covariates.

Furthermore, in other analyses presented in this work, e.g. the analysis of gene-statin interactions on A1c, we identify interaction effects whose signs are the same as the corresponding main genetic effects, and others whose signs are opposite to the corresponding main effects. This result is not consistent with the discussed generative model, where endogeneity bias manifests as interaction effects whose signs are determined by the corresponding main genetic effects—they are either all the same as the main effects or opposite to them. This is a further indication that our approach to analyzing cross-sectional data can generate valid hypotheses on genetic modifiers and statistical predictions for treatment response.

However, we do note that endogeneity induced through other generative processes may not have the same interaction effect property and it is a shortcoming of our approach.

### 3.3.1 Simulating endogenous ‘E’

Here, we perform simulations to understand a particular form of endogeneity that is surely present in our analyses: statins are prescribed for individuals with higher levels of LDL cholesterol. We are concerned with the impact of this endogeneity on our gene-drug interaction tests in the absence of any genetic interactions at baseline. Therefore, we simulate LDL cholesterol as a purely additive genetic trait, as is standard in complex trait genetics:

$$\begin{aligned} y &\sim G\beta + \epsilon \\ \beta_l &\stackrel{\text{iid}}{\sim} \mathcal{N}(0, \sigma_g^2/L) \\ \epsilon_l &\stackrel{\text{iid}}{\sim} \mathcal{N}(0, \sigma_e^2) \end{aligned}$$

We use  $N = 10,000$  samples,  $L = 100$  SNPs,  $\sigma_g^2 = .5$ , and  $\sigma_e^2 = .5$ . Note that this is a special case of our GxEMM model, where  $V = 0$  and  $W = \sigma_e^2 I_2$ . That is, the genetic heterogeneity is absent, and the noise is i.i.d. across contexts.

The novel part of our simulation is adding a drug effect in a way that depends on  $y$ . Specifically, we assume the drug ( $E$ ) is administered to individuals above the 80th percentile of the LDL cholesterol distribution. We consider two different models for the drug effect:

- Homogeneous across individuals. In this case, the phenotype  $y$  is modified by:

$$y \leftarrow y + E\beta_E$$

where  $E$  is a 0-1 indicator of drug use status, and we take  $\beta_E = -1$ . (This is one standard deviation on the pre-treatment phenotype scale.)

- Projecting individuals to the treatment threshold: all individuals with  $y_i$  above the threshold are returned directly to the threshold.

These operations are visualized in the post-treatment phenotype histograms in the left column of Figure S2. These two scenarios are intended to represent two different realistic treatment effects: in the homogeneous case, everyone gets the same effect; in the threshold case, everyone is given a drug dosage/regimen to achieve a target phenotype.

After simulating the data, we then perform a series of regressions to understand the impact on effect size estimates. First, we compare the additive genetic effects (from regressing post-treatment phenotypes on  $G$ ) to the interaction genetic effects (the interaction term from regression post-treatment phenotypes on  $G \times E$ ). As expected based on our real data analyses in Figure S5, we find that GxE effects are starkly negatively correlated with additive effects (second column of Figure S2). This reflects systematic buffering of genetic effects after treatment, which can also be seen when we compare the effect size estimates from only treated vs only untreated individuals (third column of Figure S2). Finally, we observe that the additive effect estimates are modestly reduced when fitted to post-treatment phenotypes rather than pre-treatment phenotypes (fourth column).

We next fit GxEMM with HE regression to estimate  $h^2(\Delta y)$  from the same simulations (with the Homogeneous ‘E’ effect for simplicity). We found that  $h^2(\Delta y)$  was 13.8% under this model (on average over 100 simulations, standard error=0.6%). These simulations assume that baseline LDL cholesterol has heritability of 50%. When we instead assume baseline heritability of 20%, we found that  $h^2(\Delta y)$  was 4.3% (on average over 100 simulations, standard error=0.4%). Qualitatively, these results are consistent with the observed  $h^2(\Delta y)$  for the LDL cholesterol response to statins that we observe in practice (9%) because the LDL cholesterol heritability likely lies in the range of 20-50%.

### 3.4 The impact of gene-drug interactions on polygenic prediction accuracy

We assessed transferability of PGSs between samples that are of similar genetic ancestry but differ by the drug use status.

We used four samples for training: 1. drug users (50% of all users of a given drug), 2. non-users (randomly subsampled to match the size of sample 1), 3. a 50:50 mixture of users and non-users (randomly subsampled to together match the size of sample 1), 4. merged samples 1 and 2.

We call the PGSs trained in samples 1 and 2, “on-drug-PGS” and “off-drug-PGS”, respectively. We trained two PGSs using sample 3: “agnostic-PGS”, where we used the standard covariates (age, sex, birth date, Townsend deprivation index, and the first 16 genetic PCs), and “adjusted-PGS”, where we added the drug use status to the standard covariates. The drug use status was also added when training PGSs in sample 4, which we call “adjusted-all-PGS”.

We fitted PGSs using a fast implementation of penalized linear regression with the lasso penalty [S12, S13], and we measured prediction accuracy by the incremental  $R^2$  over baseline covariates (Table S9). Standard errors around the estimates were calculated using bootstrap.

We also calculated the incremental  $R^2$  for models including more than one PGS as regressors: 1) on-drug-PGS and off-drug-PGS, and 2) on-drug-PGS, off-drug-PGS and adjusted-all-PGS (Table S9).

## Supplemental References

- S1. Dahl, A., Nguyen, K., Cai, N., Gandal, M. J., Flint, J., and Zaitlen, N. (2020). A Robust Method Uncovers Significant Context-Specific Heritability in Diverse Complex Traits. *American Journal of Human Genetics* 106, 71–91. 10.1016/j.ajhg.2019.11.015.
- S2. Yang, J. et al. (2010). Common SNPs explain a large proportion of the heritability for human height. *Nature Genetics* 42, 565–569. 10.1038/ng.608.
- S3. Robinson, M. R. et al. (2017). Genotype-covariate interaction effects and the heritability of adult body mass index. *Nature Genetics* 49, 1174–1181. 10.1038/ng.3912.
- S4. Ni, G., Werf, J. van der, Zhou, X., Hyppönen, E., Wray, N. R., and Lee, S. H. (2019). Genotype-covariate correlation and interaction disentangled by a whole-genome multivariate reaction norm model. *Nature Communications* 10, 1–15. 10.1038/s41467-019-10128-w.
- S5. Weissbrod, O., Flint, J., and Rosset, S. (2018). Estimating SNP-Based Heritability and Genetic Correlation in Case-Control Studies Directly and with Summary Statistics. *American Journal of Human Genetics* 103, 89–99. 10.1016/j.ajhg.2018.06.002.
- S6. Yang, J., Lee, S. H., Goddard, M. E., and Visscher, P. M. (2011). GCTA: A tool for genome-wide complex trait analysis. *American Journal of Human Genetics* 88, 76–82. 10.1016/j.ajhg.2010.11.011.
- S7. Gamazon, E. R. et al. (2015). A gene-based association method for mapping traits using reference transcriptome data. *Nature Genetics* 47, 1091–1098. 10.1038/ng.3367.
- S8. Gusev, A. et al. (2016). Integrative approaches for large-scale transcriptome-wide association studies. *Nature Genetics* 48, 245–252. 10.1038/ng.3506.
- S9. Almli, L. M., Duncan, R., Feng, H., Ghosh, D., Binder, E. B., Bradley, B., Ressler, K. J., Conneely, K. N., and Epstein, M. P. (2014). Correcting systematic inflation in genetic association tests that consider interaction effects application to a genome-wide association study of posttraumatic stress disorder. *JAMA Psychiatry* 71, 1392–1399. 10.1001/jamapsychiatry.2014.1339.
- S10. Cornelis, M. C., Tchetgen, E. J., Liang, L., Qi, L., Chatterjee, N., Hu, F. B., and Kraft, P. (2012). Gene-environment interactions in genome-wide association studies: A comparative study of tests applied to empirical studies of type 2 diabetes. *American Journal of Epidemiology* 175, 191–202. 10.1093/aje/kwr368.
- S11. Tchetgen, E. J. and Kraft, P. (2011). On the robustness of tests of genetic associations incorporating gene-environment interaction when the environmental exposure is misspecified. *Epidemiology* 22, 257–261. 10.1097/EDE.0b013e31820877c5.
- S12. Privé, F., Aschard, H., and Blum, M. G. B. (2019). Efficient Implementation of Penalized Regression for Genetic Risk Prediction. *Genetics* 212, 65–74. 10.1534/genetics.119.302019.
- S13. Privé, F., Aschard, H., Carmi, S., Folkersen, L., Hoggart, C., O'Reilly, P. F., and Vilhjálmsson, B. J. (2022). Portability of 245 polygenic scores when derived from the UK Biobank and applied to 9 ancestry groups from the same cohort. *American Journal of Human Genetics* 109, 12–23. 10.1016/j.ajhg.2021.11.008.
- S14. Oni-Orisan, A., Haldar, T., Ranatunga, D. K., Medina, M. W., Schaefer, C., Krauss, R. M., Iribarren, C., Risch, N., and Hoffmann, T. J. (2020). The impact of adjusting for baseline in pharmacogenomic genome-wide association studies of quantitative change. *npj Genomic Medicine* 5. 10.1038/s41525-019-0109-4.